Calculation of Shielding Effectiveness of an Apertured Rectangular Cavity Against Planar Electromagnetic Pulses

Xiaoning Shi, Chongqing Jiao, and Shuai Niu
State Key Laboratory of Alternate Electrical Power System with Renewable Energy Sources
North China Electric Power University, Beijing 102206, China

Abstract— Based on the equivalent circuit method and the Fourier transform technique, an approximate analytical model for calculating the shielding effectiveness of an apertured rectangular cavity against planar electromagnetic pulse is presented. The validity of the theoretical model is verified by the comparison with the full-wave electromagnetic simulation software CST. The effects of the aperture's shape and size, and pulse width on the pulse shielding effectiveness are analyzed.

1. INTRODUCTION

Electromagnetic pulse is a kind of transient electromagnetic phenomenon characterizing wideband and high field intensity. Electromagnetic pulses, which usually are resulted from some transient processes like lightning, static discharge, high altitude nuclear burst, switching operation and circuit faults, may couple into electronic equipment and systems via antenna, hole, cable, etc., and then cause the performance degrade of the equipment and systems. With the development of wireless communication technology, high-speed circuit and extensive application of microelectronic device, the sensitivity of the electrical and electronic equipment to electromagnetic pulse is increasing continuously. The electromagnetic interference protection problem has received widespread attention [1–5].

Electromagnetic shielding is one of the most basic methods to suppress electromagnetic interference, and its common form is isolating the sensitive equipment using shielding shell made of metal materials to prevent the entry of external electromagnetic disturbance or the leakage of internal electromagnetic disturbance. Completely closed metal cavity has very high shielding effectiveness for electromagnetic fields except low frequency magnetic field. In practice, there exist a large number of holes on the shield for some indispensable functions like ventilation and heat dissipation. In general, the electromagnetic field penetrating directly through the metal wall of a shield can be neglected. Therefore, the hole on the shield is the dominant way for the coupling between the internal and external region of the shield, and hence is the key factor affecting the shielding effectiveness (SE) of a shield. So, lots of works focus their attention on the effect of apertures on shielding effectiveness, and some numerical [4–7], analytical [10–12] or experimental techniques [8–11] have been presented to solve the problem.

Although numerical method on this issue is widely applied, but its complexity, high computational cost [14–16] make the development of analytic method of easy implementation, quick calculation and clear physical meaning still necessary. For harmonic field, people have put forward the equivalent circuit method and analytical method based on the Bethe holes coupling theory and mode expansion theory [17–19]. For the non-harmonic field, relevant analytic theory model is rarely reported.

In this paper, a novel model is proposed to calculate the SE of an apertured cavity against electromagnetic pluses. The model is the combination of the frequency-domain equivalent circuit model reported in Ref. [8] and the Fourier transform technique. First, we transform the incident pulse signal in time domain into frequency domain. Second, equivalent circuit model is used to calculate the electromagnetic field in the cavity in frequency domain. Third, the waveform in time domain is obtained by using Fourier inverse transform. To test the validity of this model, the calculation results of the simulation software CST are also presented. The effects of the size and shape of the hole, and pulse width on the cavity shielding effectiveness are also analyzed.

2. THEORETICAL MODEL

Figure 1 shows an apertured rectangular enclosure under the illumination of planar electromagnetic pulses. The height, length and depth of the enclosure are denoted by a, b, and d, respectively. The wall of the enclosure is assumed to be perfect conducting and has a thickness of t. There is a rectangular aperture of length l and width w on the left wall of the enclosure. The point P_1 is

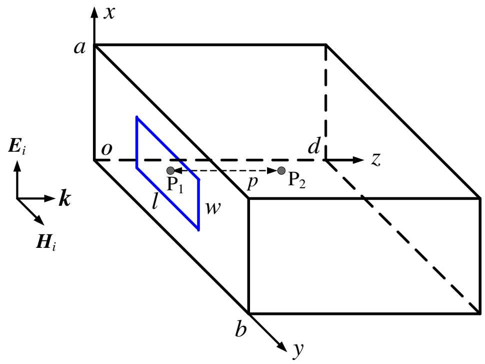

Figure 1: Apertured rectangular enclosure against planar electromagnetic pulses.

the center of the aperture and P_2 represents the point where the shielding effectiveness will be observed.

The electric shielding effectiveness S_E at a given point is defined as the ratio of the maximum electric field intensity of the time domain E_0 at the point with the enclosure removed to the maximum electric field intensity E_s at the same point with the shield applied.

$$S_E = 20 \log_{10} \left| \frac{E_0}{E_s} \right| \tag{1}$$

Similarly, the magnetic shielding effectiveness S_H is defined as

$$S_H = 20 \log_{10} \left| \frac{H_0}{H_s} \right| \tag{2}$$

The shielded field E_s and H_s can be calculated by the equivalent circuit in Fig. 2, Where the incident plane wave is represented by voltage V_0 and impedance $Z_0 = 377\,\Omega$.

The aperture is treated as a coplanar strip transmission line with a length of l along the y axis, shorted at each end. Then, the effect of the aperture can be embodied by the shunt impedance Z_{ap} in the circuit model with [8].

$$Z_{ap} = \frac{j}{2}\frac{l}{a}120\pi^2 \left[\ln \left(2\frac{1+\sqrt[4]{1-(w_e/b)^2}}{1-\sqrt[4]{1-(w_e/b)^2}} \right) \right]^{-1} \tan \frac{k_0 l}{2} \tag{3}$$

where $k_0 = 2\pi/\lambda$, and $w_e = w - (5t/4\pi)\left[1 + \ln(4\pi w/t)\right]$.

The enclosure is considered as a rectangular waveguide with a length of d along the z axis and shorted at the right end ($z = d$). When the wave frequency is lower than the cutoff frequency of the second lowest mode of the waveguide, we can assume there is only a single mode of propagation, that is, the TE_{10} mode. Then, the waveguide can be modeled very well by a transmission line with its characteristic impedance $z_g = \eta_0/\sqrt{1-(\lambda/2a)^2}$ and propagation constant $k_g = k\sqrt{1-(\lambda/2a)^2}$.

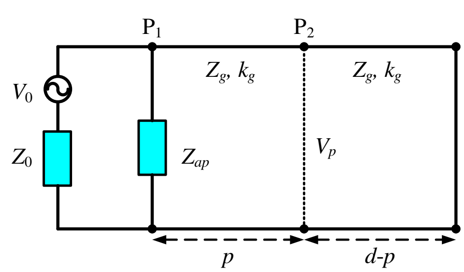

Figure 2: The equivalent circuit model for the apertured rectangular enclosure against planar electromagnetic pulses.

For the Gaussian excitation case, the time domain expression of plane wave electromagnetic pulse is $f_i(t)$. We can obtain its expression in frequency domain by Fourier transform.

$$F(\omega) = \int_{-\infty}^{+\infty} f_i(t) e^{-j\omega t} dt \tag{4}$$

This expression is used as the voltage source V_0 of equivalent circuit. By Thevenin's equivalent circuit theorem, combining V_0, Z_0 and Z_{ap} gives an equivalent voltage V_1 and source impendence Z_1.

$$V_1 = V_0 \frac{Z_{ap}}{Z_{ap} + Z_0} \tag{5}$$

$$Z_1 = \frac{Z_{ap} Z_0}{Z_{ap} + Z_0} \tag{6}$$

We now transform V_1, Z_1, and the short circuit at the end of the waveguide to P_2, giving an equivalent voltage V_2, source impendence Z_2, and load impendence Z_3.

$$V_2 = \frac{V_1}{\cos k_g p + j (Z_1/Z_g) \sin k_g p} \tag{7}$$

$$Z_2 = \frac{Z_1 + j Z_g \tan k_g p}{1 + j (Z_1/Z_g) \tan k_g p} \tag{8}$$

$$Z_3 = j Z_g \tan k_g (d - p) \tag{9}$$

The voltage and current at P_2 in frequency domain is now

$$V_p = V_2 \frac{Z_3}{Z_2 + Z_3} \tag{10}$$

$$I_p = \frac{V_2}{Z_2 + Z_3} \tag{11}$$

Then the unilateral Fourier inverse transform is used to get the time-domain expression of electric field and magnetic field in the cavity.

$$f_E(t) = \frac{1}{\pi} \int_0^{+\infty} \mathrm{Re}\left[V_p(\omega) e^{j\omega t}\right] d\omega \tag{12}$$

$$f_H(t) = \frac{1}{\pi} \int_0^{+\infty} \mathrm{Re}\left[I_p(\omega) e^{j\omega t}\right] d\omega \tag{13}$$

The maximum of $f_E(t)$ is E_S, and the maximum of $f_i(t)$ is E_0. The maximum of $f_H(t)$ is H_S, and the ratio of the maximum of $f_i(t)$ and Z_0 is H_0. All of the electric fields calculated are in the direction of x axis and the magnetic fields are in the direction. of y axis.

3. WAVEFORM OF ELECTRIC AND MAGNETIC FIELDS IN THE CAVITY

3.1. The Electric Field Waveform

The time domain expression of the incident plane wave electromagnetic pulse (Gaussian pulse) is

$$f_i(t) = e^{-u(t-t_0)^2} \tag{14}$$

The value of u are 1×10^{17}, 7×10^{17}, $1 \times 10^{18}\,\mathrm{s}^{-2}$, respectively. The spectrum of the incident Gaussian pulse is shown in Fig. 3. The dimensions of the enclosure employed for calculation are: $a = 30\,\mathrm{cm}$, $b = 12\,\mathrm{cm}$, $d = 30\,\mathrm{cm}$, $t = 1.5\,\mathrm{mm}$, $l = 5\,\mathrm{mm}$ and $w = 5\,\mathrm{mm}$. Figs. 4–6 plots the curves of the electric field waveform at the center of the cavity ($p = 15\,\mathrm{cm}$) for the three different values of u.

Figure 4 shows that when u is $1 \times 10^{17}\,\mathrm{s}^{-2}$, the electric field strength is zero before $t = 5\,\mathrm{ns}$. From about $t = 5\,\mathrm{ns}$ to $t = 20\,\mathrm{ns}$, the waveform is approximately a complete sine wave, and then goes to zero. The second half of the sine wave is actually the reflection of the first half of wave at

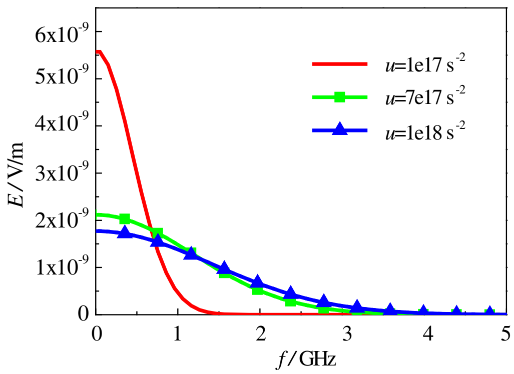

Figure 3: Frequency spectrum of Gaussian pulses.

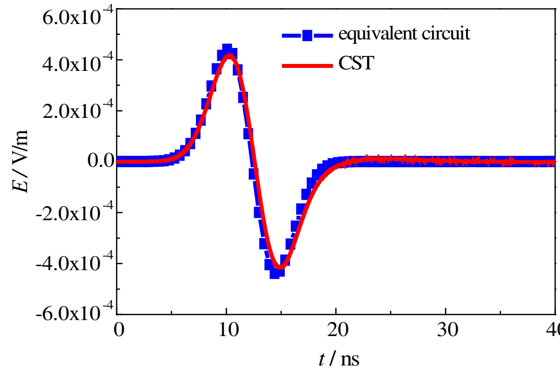

Figure 4: Time domain waveform at the center of the enclosure against planar electromagnetic pulses ($u = 1 \times 10^{17}\,\mathrm{s}^{-2}$, $t_0 = 12\,\mathrm{ns}$).

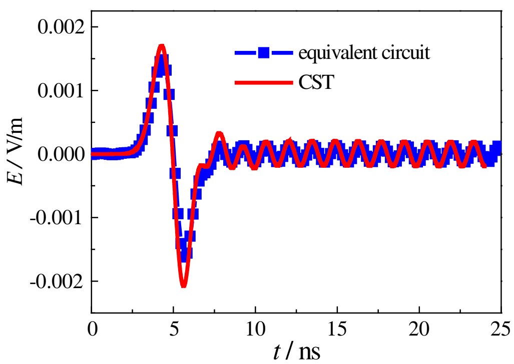

Figure 5: Time domain waveform at the center of the enclosure against planar electromagnetic pulses ($u = 7 \times 10^{17}\,\mathrm{s}^{-2}$, $t_0 = 5\,\mathrm{ns}$).

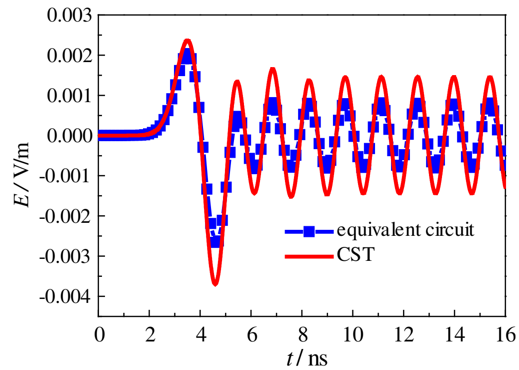

Figure 6: Time domain waveform at the center of the enclosure against planar electromagnetic pulses ($u = 1 \times 10^{18}\,\mathrm{s}^{-2}$, $t_0 = 4\,\mathrm{ns}$).

the back of the cavity wall. When u increases to $7 \times 10^{17}\,\mathrm{s}^{-2}$, the Fig. 5 shows that the waveform of electric field intensity contains not only a single period of the sine wave of high amplitude, but also a sinusoidal steady state response of low amplitude. The frequency of the steady state response is 0.7 GHz which is resulted from the resonance of the TE_{101} cavity mode. There are two aspects of the impact for the increase of the high frequency components caused by the increase of u. On the one hand, it makes the maximum value of the electric field inside the cavity increases, and the shielding effectiveness of the cavity reduces. On the other hand, it will also stimulate the resonance mode of the cavity forming the steady-state oscillation.

As is shown in Fig. 6, when u increases to $1 \times 10^{18}\,\mathrm{s}^{-2}$, the maximum of electric field strength increases further, and the amplitude of the steady-state response of increases as well. When u is small, our method has a good agreement with the computational result of CST software (Figs. 4 and 5). When u is bigger, the two results are in good agreement in the time synchronization, but there is a little difference in the amplitude. The reason is that the frequency component more than 1 GHz appears in great quantities, making higher order waveguide modes (such as TE_{20} mode whose cutoff frequency is 1 GHz) can't be ignored, while only the influence of the TE_{10} mode is considered in this paper. It should be noted that all of the TE_{10n} cavity modes are incorporated in the present model, since they can be regarded as the different spatial distribution forms of TE_{10} waveguide mode along the z axis.

3.2. The Magnetic Field Waveform

The Gaussian pulse parameter u is set to be $1 \times 10^{18}\,\mathrm{s}^{-2}$, and the magnetic field waveform at $p = 0.15\,\mathrm{m}$ and $p = 0.25\,\mathrm{m}$ are calculated respectively, as is shown in Fig. 7 and Fig. 8.

From Fig. 7 we can see that the magnetic field strength waveform at $p = 0.15\,\mathrm{m}$ in the cavity has only a large positive pulse wave with neither a large negative pulse nor a periodic oscillation following up, which are very different from the electric field waveform in Fig. 6. The reason is that when reflecting after encountering the back wall of the cavity, the direction of the electric field

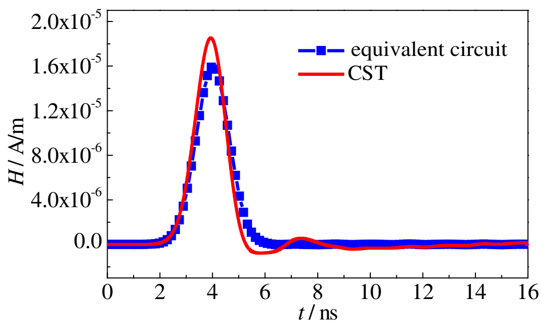

Figure 7: Time domain waveform of the magnetic field ($p = 0.15\,\mathrm{m}$).

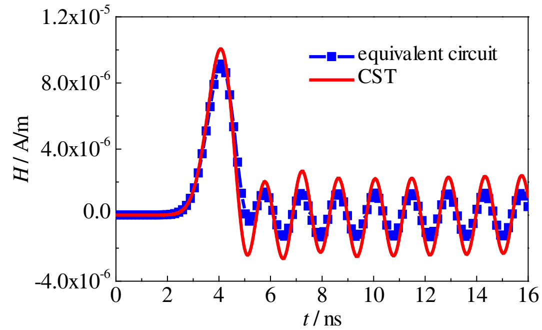

Figure 8: Time domain waveform of the magnetic field ($p = 0.25\,\mathrm{m}$).

will reverse, while the direction of the magnetic field will not. Thereby, for the electric field, the reflected wave and incident wave are superimposed in the same direction, and because of the lag in the former, the waveform with a positive pulse part and a negative pulse part is formed. As to the magnetic field, the reflected wave and incident wave are superimposed in the opposite direction, but there are not enough time intervals to form two separate parts of waveform. The reason why there is also no subsequent periodic oscillation is not that no TE_{101} resonance is formed, but the oscillation is in the standing wave form, and the center of cavity just is the node of the standing wave. For the point of $p = 0.25\,\mathrm{m}$, which is not the node of standing wave, the magnetic field waveform contains a periodic steady state response of 0.7 GHz as shown in Fig. 8.

4. CALCULATION OF SHIELDING EFFECTIVENESS

Take the parameter u of the Gaussian pulse plane wave for $1 \times 10^{18}\,\mathrm{s}^{-2}$, and shielding effectiveness at the center of the cavity with different apertures and pulse width is analyzed.

4.1. Different Size of the Aperture

Assume that the shape of the aperture is square. Shielding effectiveness at the center of the cavity with different size of the aperture is shown in Fig. 9. As you can see, SE decreases with the increasing the side length. Our calculated results and the simulation results match well when the side length of the aperture is about 23 mm. while the aperture is bigger or smaller, there is a little difference which is less than 10 dB.

4.2. Different Shape of the Aperture

Figure 10 shows the SE at the center of the cavity versus the length a when the area of the aperture is fixed at $16\,\mathrm{cm}^2$. We can see that the shape also affects the shielding effectiveness, which is decrease with the increasing of the length of the long side. Therefore, in order to get good shielding effectiveness, seam and slim aperture should be avoided. And the shape of the aperture should be square or circular. The calculation results of equivalent circuit are slightly larger than the simulation results, but the maximum difference is within 8 dB.

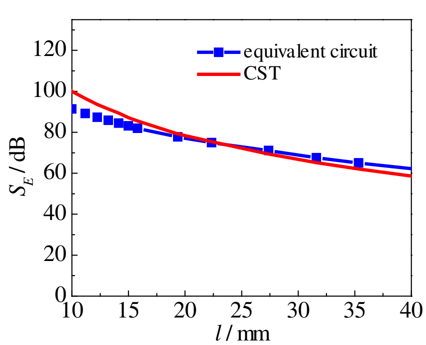

Figure 9: SE for different size of the square aperture.

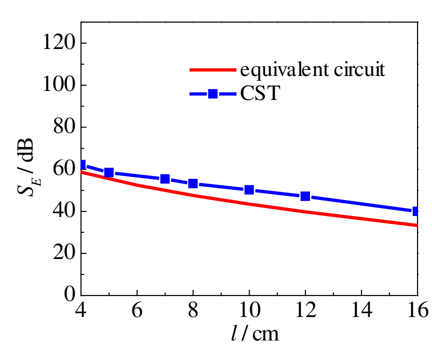

Figure 10: Dependence of the SE on the length of the aperture.

4.3. Different Pulse Width

Figure 11 shows the shielding effectiveness of the cavity with certain aperture parameters ($l = 0.1\,\mathrm{m}$, $w = 0.05\,\mathrm{m}$) while the parameter u changes.

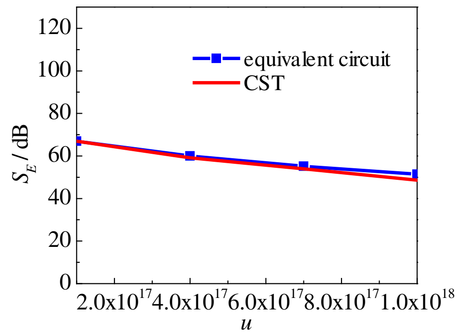

Figure 11: SE for the different values of u.

As can be seen from Fig. 11, shielding effectiveness is falling with the increase of u. It's because of the increasing of the high frequency components. And the calculation results of equivalent circuit method and CST match very well.

5. CONCLUSION

Based on the frequency domain equivalent circuit method, and combining the time-frequency domain conversion of the Fourier transform, an analytical model is established to calculate SE in an apertured rectangular cavity against planar electromagnetic pulses is established. This model is characterized by simple implementation, fast computing speed, and its calculation results are consistent with the calculation results of electromagnetic simulation software CST. Take Gaussian pulse as an example, the electric and magnetic field in the cavity in time domain is analyzed. Also, the influence of size and shape of the capture and pulse width on the shielding effectiveness is also revealed. It is shown that the electromagnetic response in the cavity contains transient part and steady part. The former is mainly composed of the incident wave and the reflected wave, and the latter is due to the resonance modes. When the width of Gaussian pulse spectrum is small, there is no steady-state response. With the increasing of the size and length of the aperture and width of Gaussian pulse spectrum, shielding effectiveness of the cavity will decrease. Higher order modes, transmission and polarization direction of incident wave are not consider in this model, the influence of these factors can be resolved by superposition of the modes and decomposition of the incident field in future work.

REFERENCES

1. Faghihi, F. and H. Heydari, "Reduction of leakage magnetic field in electromagnetic systems based on active shielding concept verified by eigenvalue analysis," *Progress In Electromagnetics Research*, Vol. 96, 217–236, 2009.
2. Wang, Y. J., W. J. Koh, C. K. Lee, and K. Y. See, "Electromagnetic coupling analysis of transient signal through slots or apertures perforated in a shielding metallic enclosure using FDTD methodology," *Progress In Electromagnetics Research*, Vol. 36, 247–264, 2002.
3. Xu, X. and X. Yang, "A hybrid formulation based on unimoment method for investigating the electromagnetic shielding of sources within a steel pipe," *Progress In Electromagnetics Research*, Vol. 12, 133–157, 1996.
4. Harrington, R. F. and J. R. Mautz, "Characteristic modes for aperture problems," *IEEE Trans. Microw. Theory.*, Vol. 33, No. 6, 500–505, Jun. 1985.
5. Audone, B. and M. Balma, "Shielding effectiveness of apertures in rectangular cavities," *IEEE Transactions on Electromagnetic Compatibility*, Vol. 31, No. 1, 102–106, Feb. 1989.
6. Wang, T., R. F. Harrington, and J. R. Mautz, "Electromagnetic scattering from and transmission through arbitrary apertures in conducting bodies," *IEEE Trans. Antennas Propag.*, Vol. 38, No. 11, 1805–1814, Nov. 1990.
7. Ma, K. P., M. Li, J. L. Drewniak, T. H. Hubing, and T. P. Van Doren, "Comparison of FDTD algorithms for subcellular modelding of slots in shielding enclosures," *IEEE Transactions on Electromagnetic Compatibility*, Vol. 39, No. 2, 147–155, May 1997.

8. Robinson, M. P., T. M. Benson, C. Christopoulos, J. F. Dawson, M. D. Ganley, A. C. Marvin, S. J. Porter, and D. W. P. Thomas, "Analytical formulation for the shielding effectiveness of enclosures with apertures," *IEEE Transactions on Electromagnetic Compatibility*, Vol. 40, No. 3, 240–248, Aug. 1998.
9. Shim, J. J., D. G. Kam, J. H. Kwon, and J. Kim, "Circuital modeling and measurement of shielding effectiveness against oblique incident plane wave on apertures in multiple sides of rectangular enclosure," *IEEE Transactions on Electromagnetic Compatibility*, Vol. 52, No. 3, 566–577, Aug. 2010.
10. Jiao, C. Q., "Shielding effectiveness improvement of metallic waveguide tube by using wall losses," *IEEE Transactions on Electromagnetic Compatibility*, Vol. 54, No. 3, 696–699, Jun. 2012.
11. Dehkhoda, P., A. Tavakoli, and R. Moini, "An efficient and reliable shielding effectiveness evaluation of a rectangular enclosure with numerous apertures," *IEEE Transactions on Electromagnetic Compatibility*, Vol. 50, No. 1, 208–212, Feb. 2008.
12. Solin, J. R., "Formula for the field excited in a rectangular cavity with a small aperture," *IEEE Transactions on Electromagnetic Compatibility*, Vol. 53, No. 1, Feb. 2011.
13. Nie, B. L., P. A. Du, Y. T. Yu, and S. Zheng, "Study of the shielding properties of enclosures with apertures at higher frequencies using the transmission-line modeling method," *IEEE Transactions on Electromagnetic Compatibility*, Vol. 53, No. 1, 73–81, 2011.
14. Chen, J. and J. G. Wang, "A three-dimensional semi-implicit FDTD scheme for calculation of shielding effectiveness of enclosure with thin slots," *IEEE Transactions on Electromagnetic Compatibility*, Vol. 49, No. 2, 354–360, 2007.
15. Wallyn, W., D. D. Zutter, and H. Rogier, "Prediction of the shielding and resonant behavior of multi section enclosures based on magnetic current modeling," *IEEE Transactions on Electromagnetic Compatibility*, Vol. 44, No. 1, 130–138, 2002.
16. Fan, Y. P., Z. W. Du, and K. Gong, "Analysis on shielding effectiveness of rectangular cavity perforated with a single slot," *Journal of Electronics* & *Information Technology*, Vol. 27, No. 12, 2005.
17. Nitsch, J. B., S. V. Tkachenko, and S. Potthast, "Transient excitation of rectangular resonators through electrically small circular holes," *IEEE Transactions on Electromagnetic Compatibility*, Vol. 54, No. 6, 1252–1259, 2012.
18. Jiao, C. Q. and L. Qi, "Electromagnetic coupling and shielding effectiveness of apertured rectangular cavity under plane wave illumination," *Acta Physica Sinica*, Vol. 61, No. 13, 134104–134109, 2012.
19. Azaro, R., S. Caorsi, and M. Donelli, "Evaluation of the effects of an external incident electromagnetic wave on metallic enclosures with rectangular apertures," *Microwave and Optical Tech.*, Vol. 28, No. 5, 289–293, 2001.